Aircraft fuel burn performance study: a data-enhanced modeling approach

Jefry Yanto[1], Rhea P. Liem[2]

The Hong Kong University of Science and Technology (HKUST), Hong Kong

Abstract

The rapid growth in commercial air transportation and the price volatility of fuel push for fuel reduction policy to be implemented. Some changes in technology (e.g., improved designs of aircraft and engines), operations (e.g., improved flight routes), or both have shown promising results on fuel reduction in air transportation. Several candidate policy scenarios related to fuel consumption need to be evaluated, which call for fast, efficient, yet accurate fuel burn computation methods, in particular to compute the total aggregate fuel burn given a set of flight missions. While fuel burn evaluation models exist, some are computationally expensive or built based on data that might be outdated. Others suffer from the lack of accuracy due to simplification assumptions and computations. As such, we develop a fuel burn evaluation model by combining a low-fidelity physics-based model with aircraft operation and performance data. For a more accurate fuel burn computation, especially for the climb and descent segments, we integrate the state-of-the-art Base of Aircraft Data (BADA) trajectory simulation results into the fuel burn model. This model offers enhanced accuracy compared to low-fidelity models, yet retains their computational efficiency. In this paper, a fuel burn database corresponding to 40 aircraft types is generated based on the Bureau of Transportation Statistics (BTS) flight missions' database 2015. A sample-based linear regression model is then derived for each aircraft type. The validation results show that the model can estimate the total aggregate fuel burn for each aircraft type with less than 1% prediction errors using flight mission data from 2016, and less than 6% prediction errors when compared with the actual fuel burn data corresponding to three commercial airlines in 2015 and 2016. The developed models are then used to investigate the two common simplifying assumptions in fuel burn evaluation, namely the cruise-only approximation and similar aircraft type mapping (when data pertaining to some specific aircraft types are unavailable). The results provide insight into the inaccuracies

[1]Ph.D. Candidate
[2]Assistant Professor

caused by these simplifications in fuel burn computation. For instance, the cruise-only approximation shows significant error (mostly $> 30\%$) when performed on smaller aircraft, which typically fly shorter routes. The combined computational efficiency and accuracy that these models offer would open doors to perform more computationally intensive analyses, such as sensitivity and uncertainty analyses, as well as optimization. Such analyses could be computationally prohibitive when large-scale models are used.

Keywords: Aircraft fuel burn, air transportation, flight mission analysis, regression modeling, data-enhanced modeling, unsupervised learning algorithm.

1. Background and Motivation

The advancement of numerical simulation has assisted considerably the study of many complex physical phenomena and is becoming increasingly widespread as a means to support decision-making and policy making processes (Yanto and Liem, 2017). The airline industry, as an example, relies a lot on numerical analyses and modeling in its decision making analyses. In 2006, the number of passengers carried by air transport was around 2 073 billion and it increased to 3 696 billion in 2016 (The World Bank, 2016), reflecting the rapid growth in commercial air transportation. With the expected steady increases in the demand of air transportation (ICAO, 2010) and the volatility of fuel prices (IEA, 2008), fuel economy and environmental impacts of aviation have become the main drivers in many air transportation policy and decision making processes. Therefore, these policies and decisions need to be carefully analyzed. In 2010, international aviation consumed approximately 142 million metric tonnes of fuel, resulting in 448 million metric tonnes (Mt, 1kg x 10^9) of CO_2 emissions and the fuel consumption is projected to multiply by 2.8 to 2.9 times by 2040 (ICAO, 2016). However, the United States Department of Transportation's Bureau of Transportation Statistics (BTS)[3] has shown a decreasing trend within the period 2006–2009 of the total fuel consumption. This decreasing trend is a result of some changes in technology (e.g., improved designs of aircraft engines), operations (e.g., flight route), or both. To make decisions on the best policy to implement to further reduce the total fuel consumption, several candidate policy scenarios need to be carefully evaluated and compared. For instance, which combination of new engines, improved aircraft designs or structural materials, and operational procedures could reduce the total fuel consumption the most. These evaluations require outputs from flight performance analyses, in particular the amount of fuel burned during any given flight mission (simply referred to as *fuel burn* in the remainder of this paper).

[3] TranStats, Bureau of Transportation Statistics http://www.transtats.bts.gov/

Besides accuracy, computational efficiency is an important consideration in the fuel burn model derivation, for several reasons. First, the scale and complexity of analyzing the fuel burn of the global air transportation system are immense. The simulation of all flights within one year involves over 35 million flights with approximately 350 aircraft types and thousands of input parameters (presented at Deutches Zentrum für Luft- und Raumfahrt (LDR), 2010). Second, to have a realistic evaluation, we need to carefully characterize the effects of uncertainty. To do so, one might wish to perform Monte Carlo simulations, requiring many thousands of simulations to be run. While the uncertainty analysis is beyond the scope of our current paper, computational efficiency is a key performance factor of our proposed model to enable running these simulations, which will become intractable when we use expensive, large-scale models.

There are quite a number of fuel burn prediction models available, spanning from low-fidelity to high-fidelity. The different levels of fidelity are defined based on how closely the models represent the system's physics. In general, the high-fidelity models require modeling of flight mission's the detailed trajectory , taking into account the flight condition variations to evaluate the total fuel consumption. The low-fidelity models, on the other hand, may rely on empirical models, or with simplified assumptions. For instance, the cruise segment of flight is typically used to represent the entire flight mission (Kenway et al., 2012; Liem et al., 2015a). There has always been a tradeoff between the accuracy and efficiency in any computational analysis. High-fidelity models for fuel burn computation perform accurately, however, it is typically computationally expensive and time consuming (Liem et al., 2013, 2015b). Low-fidelity models can reduce the computational time, but at the expense of accuracy (Randle et al., 2011).

Some platforms have been developed by government institutions and large organizations, such as the Federal Aviation Administration (FAA) and the European Commission (EC). FAA has led the project to develop the Aviation Environmental Design Tool (AEDT) to assess aircraft fuel burn, emissions, and noise by taking into account detailed inputs such as flight schedules, trajectories, aircraft performance model, and emission factors (AEDT, 2017). The AEDT fuel burn and emissions modules were previously known as the System for assessing Aviation's Global Emissions (SAGE) (Kim et al., 2007). The International Civil Aviation Organisation (ICAO) developed the ICAO Carbon Emission Calculator[4] to estimate the fuel burn and emissions with minimum input variables (ICAO, 2015). The calculation relies on a distance-based approach that is derived based on publicly available data. The European Organization for the Safety of Air Navigation (Eurocontrol) also developed an aircraft performance model which can be used to generate

[4]ICAO Carbon Emissions Calculator http://applications.icao.int/icec

aircraft trajectories and estimate fuel consumption named the Base of Aircraft Data (BADA) [5]. We observe, however, the limited number of aircraft and nominal takeoff weights modeled in BADA.

The aforementioned models are typically not free nor publicly available. Moreover, the data used to develop the models are often outdated and might not be available for all aircraft and engine types, especially the newer ones (Wasiuk et al., 2015). Some models are derived based on existing databases, which are not suitable to perform future projections. This will be disadvantageous when we consider the potential future scenarios in policy analysis practices. This particular limitation also applies to the fuel burn evaluation using the quick access recorder (QAR) data, since they only pertain to completed flights. When data are not available, it is common to use data corresponding to another, but similar aircraft type (similar aircraft type mapping), which might compromise the accuracy. Moreover, running the models could be computationally time consuming and inefficient. For instance, for each BADA simulation, the user needs to input the aircraft and flight information one by one (e.g., aircraft type, initial and final altitudes during climb) for each segment. While each simulation takes only a few seconds to run, it is not very practical to run the trajectory simulations for the entire mission profile (including climb, cruise, and descent) thousands of times manually to generate the fuel burn database.

Apart from the detailed models mentioned above, some researchers have developed fuel burn prediction models. These models, which will be further elaborated in Section 2, are typically physics-based models, instead of empirical models.

The main objective of this research is to develop accurate but efficient approximation model for aggregate fuel burn computation.A simple sample-based linear regression model is derived for each aircraft type to facilitate this computation. For this purpose, we first need to generate a fuel-burn database for each aircraft type. To generate the database, we consult the US flight mission data corresponding to 2015 from a publicly available database. To compute the fuel burn for each flight mission, we develop a medium-fidelity fuel burn computation method, aimed to strike a compromise between the low- and high-fidelity models. The medium-fidelity model is constructed by deriving correction factors from high-fidelity models and apply them to "correct" the low-fidelity models. We can therefore combine a limited number of the more costly high-fidelity evaluations with a larger number of inexpensive low-fidelity evaluations. With this approach, we achieve a high accuracy (up to the high-fidelity models or data we use), while maintaining the computational efficiency. In this work, we use BADA trajectory simulation results as the high-fidelity

[5] https://badaext.eurocontrol.fr/

model. However, the proposed medium-fidelity modeling approach will still apply even if we change the high- or low-fidelity models. When actual flight data are available, we can achieve higher accuracy on the derived model. Chatterji, for instance, incorporated real track data in his fuel burn estimation model (Chatterji, 2011). To model the mission profile, care must be taken for short-haul flights, as they typically do not reach the cruise altitude and descend immediately after climbing. To find the climb-descent distance ratio (and thus the maximum altitude), we also consult with the BADA simulation results. The derived regression model will allow us to efficiently compute the total fuel burn for an aircraft type. Each method developed in this work is properly validated. With the derivation of linear regression model for each aircraft type, the computational cost of computing the total aggregate fuel burn is reduced from hundreds of thousands (i.e., the number of flight missions) to just a few dozen (i.e., the number of aircraft types), resulting in a significant $\mathcal{O}\left(10^4\right)$ order of reduction.

We will also use the model to perform a study to investigate the effect of common simplifications on the fuel burn predictions. As mentioned before, a similar-aircraft mapping is often employed when the corresponding data are not available; and that a cruise-only assumption is common in various fuel burn modeling approaches. We wish to quantify the accuracy of these simplifications using our derived models. To emulate the similar-aircraft mapping, we employ an unsupervised clustering algorithm for a systematic mapping, instead of manually identifying similar aircraft types. The cruise-only assumption is compared to the segment-by-segment fuel burn prediction, and the discrepancies are evaluated. The evaluation results provide insights into the error if we use these assumptions in our calculations.

This paper starts with a brief fuel burn computation review in Section 2. We will then present our proposed approach and describe the developed fuel burn computation method, database used in the modeling, as well as the corresponding validation procedures in Section 3. The studies to investigate the accuracy of common simplifications and assumptions in fuel burn prediction modeling are then discussed in Section 4. We conclude this paper with a brief summary, conclusion, and future work in Section 5.

2. Fuel Burn Model Review

Figure 1 illustrates the "ideal" fuel burn evaluation framework, showing the assessment complexity since we need to simultaneously consider the engine and airframe designs, aircraft operation, atmospheric quantities (ambient temperature, pressure, density, and speed of sound), and airline economics (Diedrich et al., 2006). To obtain global fuel burn and emissions inventories, we need to simulate the flights of all aircraft

flown worldwide, by first obtaining the detailed fleet descriptions and flight schedules (Waitz et al., 2006). This process requires a massive amount of computation.

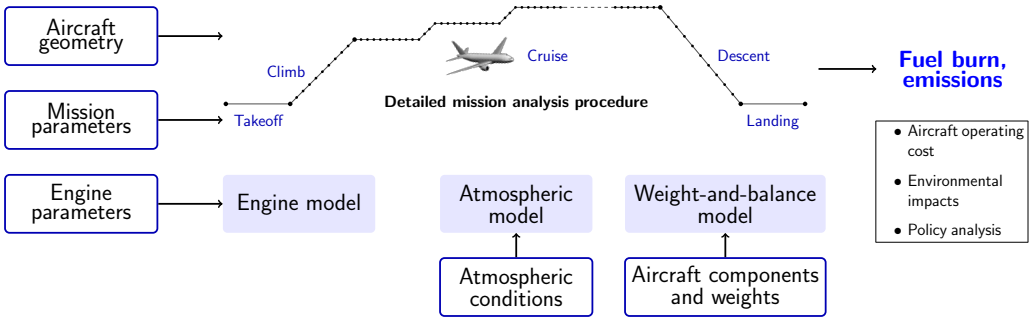

Figure 1: The disciplines involved and complexities in computing aircraft fuel burn.

Due to the aforementioned complexities and immense computational cost, aircraft fuel-burn computations are typically done with a simplification of either the physics in the model or the mission profile considered (Liem et al., 2013; Liem, 2015). Analytical and empirical models are sometimes used to reduce the computational time (Yan et al., 2012), at the expense of accuracy. Most fuel burn computations are derived based on the classical Breguet range equation (Lee et al., 2001; Randle et al., 2011; Graham et al., 2014; Singh and Sharma, 2015), which is expressed as (Coffin, 1920; Breguet, 1923):

$$R = \frac{V}{c_T}\frac{L}{D}\ln\left(\frac{W_i}{W_f}\right), \tag{1}$$

where R, V, and L/D refer to the mission range, flight speed, aerodynamic lift-to-drag ratio, respectively. The variable c_T denotes the thrust specific fuel consumption (TSFC), which is defined as the weight of fuel burned per unit time divided by the unit thrust. TSFC is a property of the aircraft engine, which is assumed constant in this work. W_i and W_f refer to the initial and final segment's aircraft weight, respectively. This equation, however, is only applicable under the assumption that TSFC, L/D, and V are constant and is more suitable to compute fuel burn during the cruise segment, and not the takeoff, climb, and descent segments (McCormick, 1979). In this work, we assume that the parameter values in Equation 1 are constant throughout a segment. This approach is therefore considered as low-fidelity. Further refinements are possible, i.e., by dividing the segment into several subsegments and varying the parameter values for each subsegment. By doing so, we will improve the accuracy of the computation. The latter approach is similar to solving the original range equation with numerical integration, as done by Liem *et al.* (Liem et al.,

2015b). To simplify fuel burn computation, it is common to use the cruise segment to represent the whole flight mission (Kenway et al., 2012; Liem et al., 2015a). Dancila *et al.* (Dancila et al., 2013) employed a higher-fidelity model to estimate the fuel burn on cruise segment. This model used the fuel burn rate time-dependent model that splits the cruise segment into sub-segments to obtain the gross weight via an iteration procedure. This approach was claimed to have more accurate performance than the Breguet range equation. Care must be taken when applying the cruise-only assumption since, while the cruise fuel burn might be dominant in long-haul flights, for short-haul flights the fuel-burn contribution from the climb segment might be too significant to be ignored (Simos and Jenkinson, 1988).

The fuel burn for other segments are typically computed using the appropriate fuel fractions (Roskam, 1985; Liem et al., 2013). Roskam (Roskam, 1985) defined the fuel fraction as the ratio between the final and initial weights on each segment. The fuel fraction values for engine start and warm-up, taxi, take-off, descent, and landing until shutdown are typically 0.99, and for the climb segment it is typically 0.985. The fuel required for each segment can then be calculated using the fuel fraction and the segment's initial and final weights. O'Kelly (O'Kelly, 2012) derived linear regression functions for the fuel burn for taxi, takeoff, cruise, and landing based on SAGE fuel burn inventory data, with distance and aircraft size as regression inputs. This model, however, does not model the fuel burn for climb and descent segments. These approaches are simple and computationally inexpensive but the result might not be sufficiently accurate.

Several efforts have been made by various researchers to include the climb and descent segments in estimating the mission's fuel burn without running trajectory simulations. Lee and Chatterji (Lee and Chatterji, 2010), for instance, further improved the fuel burn approximations for the climb and descent segments by applying a correction factor. The climb segment's fuel burn was computed by applying a correction factor to the amount of fuel required to cruise at the same distance; this correction value was represented by a fraction of the takeoff weight. The fuel burn for the descent segment was approximated with the fuel burn required to cruise the ground distance from top-of-descent to landing airport. The fuel burn for the cruise segment was computed based on the Breguet range equation, and the fuel burn for taxi, takeoff, approach and landing could be collectively approximated as a fraction of takeoff weight. A factor of 0.007 was used for the total of those phases, following the work by Kroo (Kroo, Sept 2006). The reserve fuel was expressed in fuel fraction; generally a factor of 0.08 of zero-fuel weight (Lee and Chatterji, 2010; Kroo, Sept 2006). This approach, albeit simple, improved the accuracy of the fuel prediction for the climb and descent segments. However, we observed some discrepancies in the climb and descent fuel approximations upon comparing the results to the fuel burn obtained from running flight trajectory simulations on BADA as shown in Figure 2

for one representative aircraft type (A321). During the climb segment, the Breguet range approximation underestimated the simulated fuel burn, whereas in the descent segment it was an overestimation instead. This makes sense as an aircraft burns more fuel to climb than during level flight, and would burn less fuel during descent.

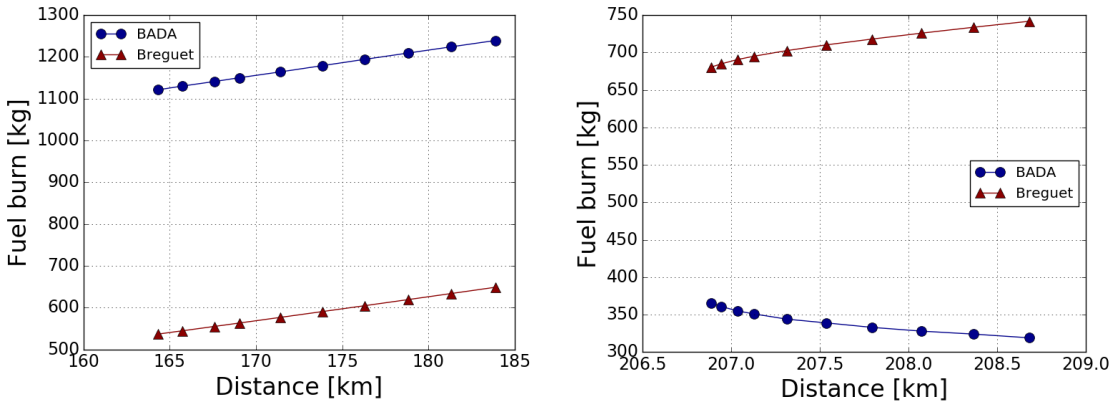

(a) Climb segment

(b) Descent segment

Figure 2: Fuel discrepancy of A321 between approximation model and BADA.

For a higher-fidelity mission analysis modeling, Liem (Liem, 2015) performed a detailed mission analysis procedure that modeled different flight conditions for the climb, cruise, and descent segments. Fuel fraction method is used to approximate the fuel burn during startup, taxi, takeoff, and landing. Solving the governing equation of each mission segment (climb, cruise, and descent) via numerical integration overcomes the limitation of low-fidelity models. This technique required the aerodynamic performance information (lift, drag, and moment coefficients) at different flight conditions along the mission profile to perform the numerical integration. With the numerical integration procedure and its iterative nature, this mission analysis procedure is computationally expensive and might take hours to complete, even with multiple processors. To reduce the required computational time, surrogate models were employed to approximate the aerodynamic performance coefficients required in the analyses. Using surrogate models offered a speedup of at least 70 times (Liem et al., 2015b), such that each flight mission analysis was completed in 6–18 minutes (depending on the mission profile) with 16 processors. Let's say we need to compute the total fuel burn of 10 000 flight missions. Using the same number of processors, this computation would take around 40 days to complete, which is impractical.

3. Proposed Fuel Burn Surrogate Modeling Approach

This section provides an overview of the proposed framework. We first provide the overview of the step-by-step procedure, before providing the details of each step.

We derive a linear regression model for each aircraft type to provide a fast approximation of the total fuel burn for any given sets of flight missions. The sample-based method is chosen due to its simplicity and non-intrusive nature. To achieve a certain level of accuracy, this technique requires a large number of samples. A medium-fidelity, data-enhanced fuel burn approximation model is derived to generate the *fuel burn database* as sample population. We use a similar approach as O'Kelly (O'Kelly, 2012) to derive the linear regression model. However, we use the fuel burn inventory generated from our developed medium-fidelity model instead of the SAGE fuel burn inventory. This procedure is summarized as follows:

Step 1 Obtain the flight mission inventories For this purpose, we select a number of aircraft types from different aircraft manufacturers and obtain the mission information of flights to and from a specific region. We used the publicly available data from the BTS T-100 Segment (All Carriers) corresponding to all flights to and from the United States in 2015 to derive the linear regression models. For each aircraft type, we gather information on the relevant parameters, mainly from the aircraft manufacturers' websites. The flight distributions for two representative aircraft (Boeing B737-800 and A320-100/200) are shown in Figure 3, with their corresponding flight envelopes in the payload-range diagram. All flights are within the flight envelopes, including those flights with longer range (where the payload capacity is less than the maximum payload due to the payload-fuel tradeoff). Therefore, the payload-fuel tradeoff is implicitly assumed in our fuel burn estimation through the data used to derive our models.

Step 2 Generate the fuel burn inventories by simulating each flight mission individually.

In this research, each flight mission is simplified into a simple mission profile as shown in Figure 4. To be realistic, we take into account all segments (takeoff, climb, cruise, descent, and landing) in flight mission including the maneuver fuel and reserve fuel. The segment-by-segment fuel burn computation will be elaborated in Section 3.3.

Step 3 Derive the linear regression model for each aircraft type.

Regression models are derived in a least-squares sense, based on the available sample-data (Liem, 2015). This technique offers simplicity and is non-intrusive. Using the fuel burn database corresponding to the BTS mission data, we derive a two-dimensional regression model to approximate fuel burn

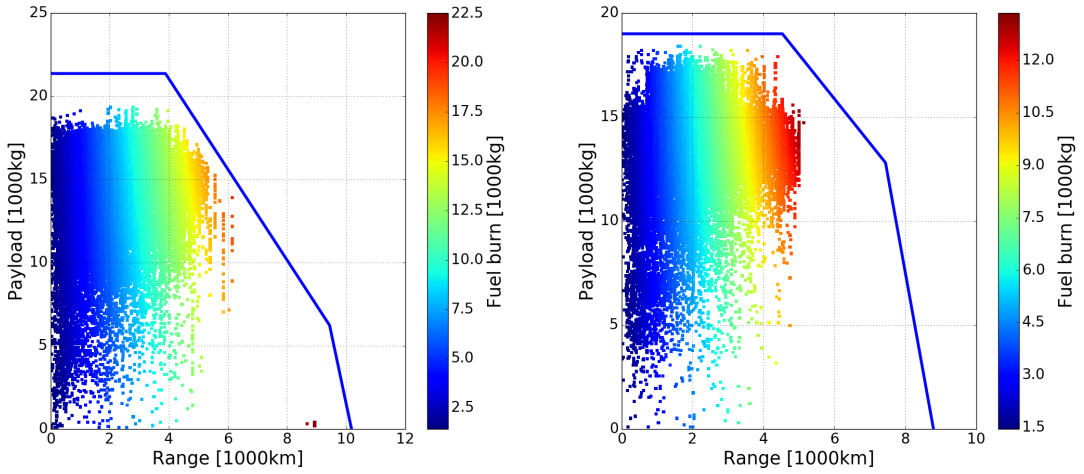

(a) Boeing B737-800

(b) Airbus A320-100/200

Figure 3: Payload range diagram.

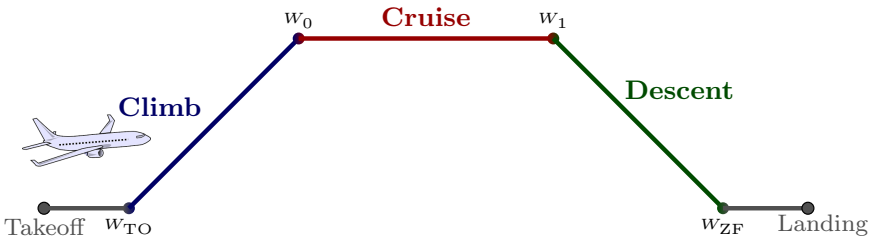

Figure 4: Simplified flight mission with five segments: takeoff, climb, cruise, descent, and landing.

for each aircraft type, using the mission payload and range as input variables. Figure 5 illustrates the Steps 1, 2, and 3 described above. This procedure is repeated for each aircraft type included in the analysis.

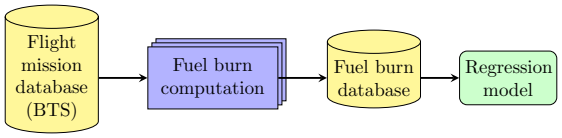

Figure 5: Fuel burn linear regression model is derived for each aircraft type, based on the fuel burn database generated for the BTS mission data.

Having presented the brief overview of our approach, we will now describe the database and some parameters that are used in this computation. Then we describe the flight mission profiles adopted in this work. We use different mission profiles for short- and long-haul flight, for reasons to be explained shortly. We then present the procedure to compute fuel burn of a flight mission, by modeling each segment separately. A regression model is then derived for each aircraft type with payload and mission-distance as input variables.

3.1. Flight mission inventories and parameter data

We obtain mission data corresponding to 40 distinct aircraft types from the US Department of Transportation BTS T-100 Segment [6], with flights going to and from the United States within the year of 2015. The flight mission information includes the distance, aircraft type, and payload information comprising the number of passengers, and weight of freight and mail. The weight information and number of passengers are used to calculate the payload by taking the summation of all carried weights. In this paper, we use the standard average of passengers weight as 225 lbs as recommended by Boeing (Baughcum et al., 1996). The use of actual aircraft operation data is intended to reflect the actual market performance of each aircraft type. This work in particular uses the US aviation data as a reference, which might not be representative of other regions or global aviation. Therefore, care must be taken when using the derived models outside the operational ranges from which the models are derived.The proposed approach, however, will still be applicable to be used with other sets of data.

[6] Bureau of Transportation Statistic (BTS), "Database Name: Air Carrier Statistics (Form 41 Traffic) – All Carriers." US Department of Transportation. https://www.transtats.bts.gov/Tables.asp?DB_ID=111&DB_Name=Air%20Carrier%20Statistics%20%28Form%2041%20Traffic%29-%20All%20Carriers&DB_Short_Name=Air%20Carriers

In addition to the flight missions, we also need to obtain some parameters corresponding to each aircraft and engine type to enable computing of the missions' fuel burn. Typically fuel flow is used to represent the engine in flight simulation models; however, in this work the fuel flow is replaced by Thrust Specific Fuel Consumption (TSFC), which is used in the Breguet range equation. At this stage, we assume the engine as single engine type for each aircraft type for simplicity, and the engine TSFC is assumed constant for the whole flight mission by taking the average values from several engine types installed in the corresponding aircraft type. Note that it might not be true in real cases, and the engine variation can be included in the future to further refine our analyses. Some other parameters are also assumed to be a constant for each aircraft type, such as zero-fuel weight, climb, cruise, and descent speed, cruise altitude, lift-to-drag ratio, and takeoff and landing distance. We use the nominal values for the cruise altitude and lift-to-drag ratio of each aircraft type for the computations performed in this work.A summary of all parameters assumed and used in this work, and their corresponding data sources, are given in Table 1.

Table 1: List of parameters used in the fuel burn computation and their sources.

Discipline	**Parameter**	**Source**
Flight mission	Payload Range Aircraft type	Bureau of Transportation Statistics (BTS)
Aircraft	Zero-fuel weight Cruise speed Cruise altitude Climb and descent speeds The lift-to-drag ratio, L/D Takeoff distance Landing distance Engine type	Aircraft manufacturers (e.g., Boeing and Airbus) websites, `http://www.airliners.net`, and `http://www.skybrary.aero`
Engine	TSFC	Engine database handbook and websites

Table 2 summarizes the aircraft parameters for the Airbus A320, as an example. These values will be used in the example computation for the segment-by-segment fuel burn calculation, which will be discussed in Section 3.3.

3.2. Mission profile

In this research, we consider different mission profiles depending on the mission range (short-haul and long-haul missions). In practice, stepped cruise is performed during the cruise segment especially for long-

Table 2: Computational time comparison between several fuel burn models.

Parameter	Value	Units
Operating empty weight (OEW)	37 500	kg
Takeoff distance	2 190	m
Landing distance	1 440	m
Climb speed	252	knots
Cruise speed	450	knots
Descent speed	250	knots
L/D	18.5	-
TSFC	0.573	N/(N · h)
Cruise altitude	35 000	ft

haul missions. However, in this paper we simplify the long-haul mission profile by dividing it into five segments as shown in Figure 4. This mission profile has been commonly used in many flight mission analysis procedures (Lee and Chatterji, 2010; Liem et al., 2013).

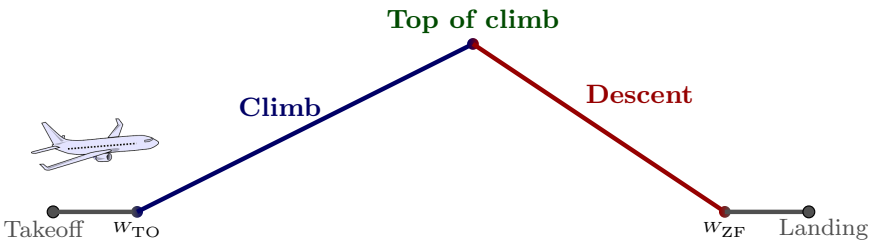

Figure 6: Simplified flight mission profile (the saw-tooth profile) for short-haul mission.

For short-haul flight mission we model the mission profile by assuming a saw-tooth profile, which is illustrated in Figure 6. This profile is more realistic and closer to the actual operation, and has previously been used by Simos and Jenkinson (Simos and Jenkinson, 1988). By using this profile, the flight path would not reach the cruise segment; instead, it goes straight to descent upon climbing. The maximum altitude before the aircraft starts descending is obtained through the triangle similarity theorem, using the climb and descent profiles of long-haul flights as reference. This theorem is illustrated in Figure 7. Essentially, we assume that the distance covered during the climb and descent segments for short-haul flights (a and b) are proportional to those of long-haul flights (x and y) for the same aircraft type. We find that the climb-descent

ratio depends on the mission payload; when the aircraft carries a heavier payload, the maximum climb altitude is lower and it needs to climb over a longer distance.

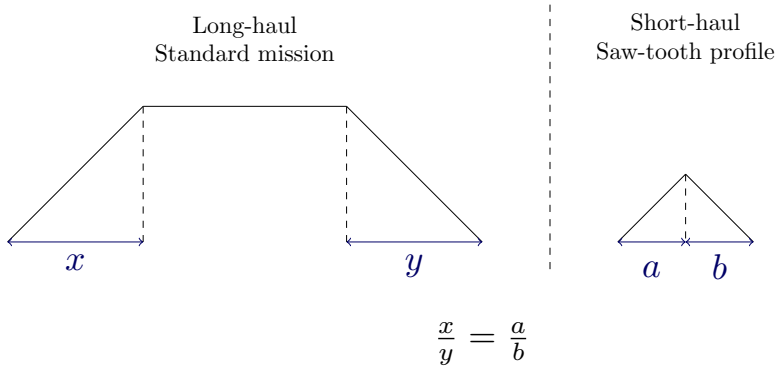

Figure 7: Triangle similarity theorem.

With the different mission profiles for short- and long-haul flights, the segment-by-segment fuel burn computation will be slightly different for the two flight types. In particular, the short-haul flight will not reach the nominal cruise altitude and thus will not have any cruise segments. In the segment-by-segment fuel burn computation procedure, we need to compute the climb and descent distances first. It will first assume the full flight mission profile (i.e., reaching the cruise altitude). We then compute the total distance covered during climb and descent. When the value is larger than the mission range, we classify the flight mission as a short-haul flight; otherwise, it is classified as a long-haul flight. This classification is highlighted in the flowchart presented in Figure 8. This flowchart also shows the step-by-step procedure, which will be explained in detail in Section 3.3. We can see that the computation steps follow different routes for short- (indicated with a red outline) and long-haul flights (indicated with a blue outline).

3.3. Segment-by-segment fuel burn computation procedure

The proposed segment-by-segment fuel burn computation procedure is illustrated in Figure 9. As inputs we have engine parameters, aircraft performance parameters, and mission parameters as listed in Table 1. BADA trajectory results are used to derive the climb and descent ranges and fuel correction factor model for these segments based on the fuel discrepancy as shown in Figure 2. Here, we use BADA as the high-fidelity model to "correct" the low-fidelity model. The accuracy of the generated medium-fidelity model is therefore limited to the accuracy of BADA. We also use Breguet range equation as the main equation to calculate the fuel burn. The output of this procedure is the fuel burn of the flight mission.

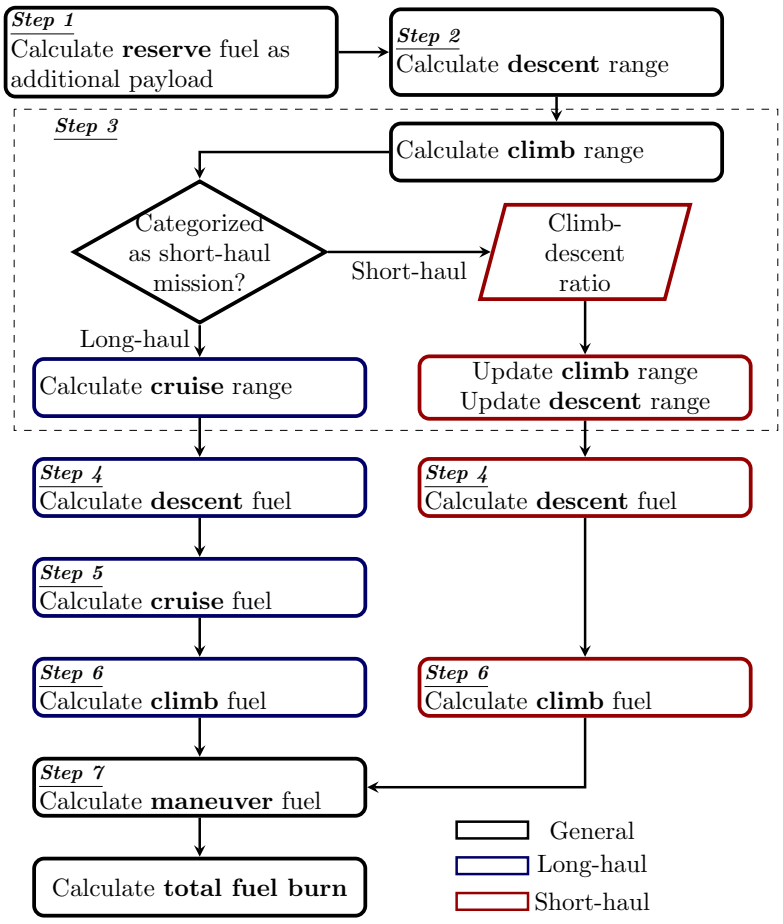

Figure 8: Segment-by-segment fuel burn computation diagram.

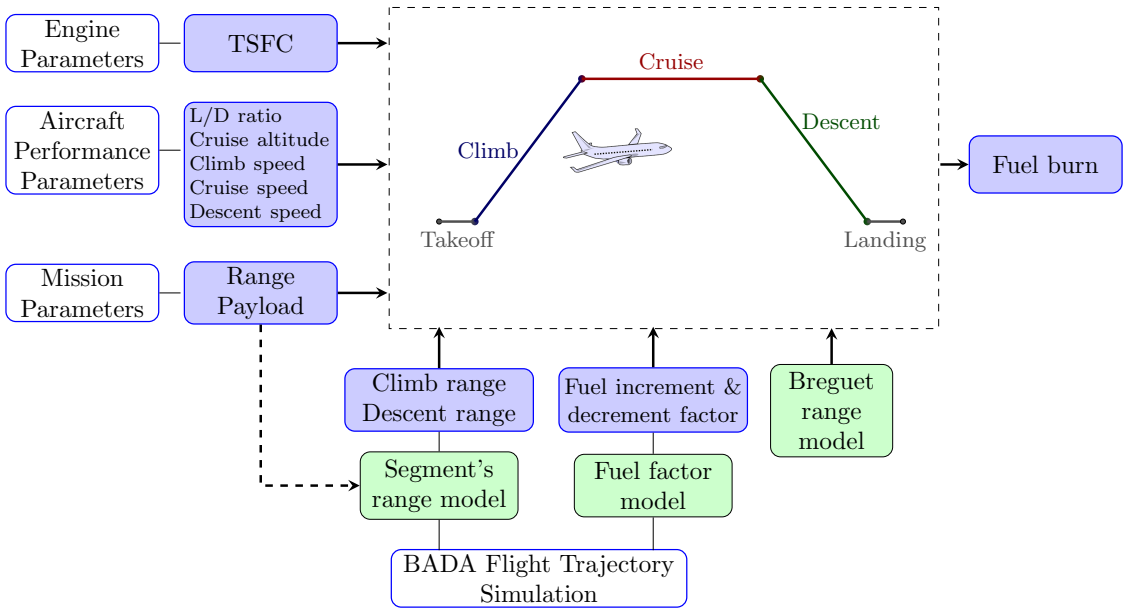

Figure 9: Proposed segment-by-segment fuel burn computation framework.

The number of flight mission samples required to derive the climb and descent fuel correction factors is determined based on some statistical measures. We use 10 samples of different payload for each aircraft type on the climb segment to derive the segment's range as well as the fuel correction factor, assuming that the climb segment reaches the cruise altitude. The descent range is derived from 10 samples of different payload for each aircraft type. To derive the descent fuel correction factor, we use 40 samples of different combination of payload and altitudes, including those lower than cruise altitude to account for short-haul flights. These samples are selected using *systematic random sampling* including the lower and upper bounds of the BADA information for each aircraft type. We use the *chi-square hypothesis test* with a confidence level of 95% to validate the sufficiency of the number of samples on deriving the climb and descent range and fuel correction factor.

The chi-square hypothesis is validated with the coefficient of variation (c_v), to validate the variability in relation to the mean of the population (Montgomery and Runger, 2003; Casella and Berger, 2001). However, we use an approach involving an unbiased estimator which is more suitable for our small sample size (Sokal and Rohlf, 2012). The unbiased estimator can be expressed as:

$$\hat{c_v}^* = \left(1 + \frac{1}{4n}\right) \hat{c_v}, \tag{2}$$

where n is the number of sample. All aircraft types have $\hat{c_v}^*$ below 3%, therefore we can assume that the data are good enough and considered as consistent (Zady). By using these correction factors, we can compute the fuel burn for the climb and descent segments with errors approximately 5% and 11% respectively.

To compute the fuel burn required for each flight mission, we consider simple mission profiles as shown in Figure 4 for long-haul flights and Figure 6 for short-haul flights. Although an aircraft typically climbs and descends through a few subsegments (i.e., accelerated climb/decelerated descent, constant velocity climb/descent, constant Mach climb/descent) (Liem et al., 2013), at this stage we combine those subsegments into one climb or one descent segment. In addition to the fuel burn during climb ($W_{\text{f, climb}}$), cruise ($W_{\text{f, cruise}}$), and descent segments ($W_{\text{f, descent}}$), the total fuel burn computation also includes the maneuver ($W_{\text{f, man}}$). The maneuver fuel is a combination of warm-up, taxi, takeoff, approach, and landing phases (Lee, 2010). The total fuel burn would then be obtained from summing up all these components, as shown below:

$$W_{\text{f}} = W_{\text{f, climb}} + W_{\text{f, cruise}} + W_{\text{f, descent}} + W_{\text{f, man}} \tag{3}$$

With this approach, the reserve fuel is considered as an additional payload and will affect the landing weight. Therefore, the computed fuel burn only refers to the fuel consumed during the flight, assuming that the reserve fuel remains unused. The procedure to compute each fuel burn component is described below, which has also been shown in Figure 8. Note that the procedure is not exactly sequential (i.e., from the first mission segment up to the last one). This is done because the fuel burn computation is interrelated, where one computation might need information from another.

Step 1 Compute the reserve fuel, which is expressed as a fixed fraction of the zero-fuel weight (W_{ZF}), with f_{res} set to 0.08 (Kroo, Sept 2006). This relation is expressed as:

$$W_{\text{f, res}} = W_{\text{ZF}} \cdot f_{\text{res}} \tag{4}$$

This fuel component will be added to mission payload. In real aircraft operation, an aircraft might also carries uplift fuel for another flight, e.g., carrying enough full for the round trip. However, in this work we assume that the aircraft only carry mission fuel and reserve fuel. The summation W_{ZF} and $W_{\text{f, res}}$ make up for the landing weight, W_{L}.

Step 2 Compute the range (ground distance) travelled during descent, R_{descent}. As shown in Figure 4, we assume the descent segment to start from the cruise altitude and end at 0 altitude. For each aircraft type, the descent range is determined by observing 10 samples of different total payload which are obtained

by running BADA flight trajectory simulations. Using these samples, we then derive the linear regression model for each aircraft type with total payload as an input variable. From the regression models, we can observe that some aircraft types exhibit a linear relationship between the descent distance and total payload, whereas for other aircraft types the relationship is nearly constant since the gradient is almost zero. Based on this observation, we differentiate two categories of aircraft types based on their descent range-and-total payload relationship. The K-means clustering algorithm is employed to divide the aircraft type into two groups. From the results, we observe that the bigger aircraft (e.g. Airbus A340, Boeing B777) tend to have constant descent ranges, whereas the smaller ones (e.g Canadair RJ-700, Embraer 140) have stronger linear relationships. The dependence between the descent range and payload is stronger for the smaller aircraft, as the payload weight takes up greater portion of the total weight compared to the larger aircraft. Thus, its effect is more notable. Each group is validated with the standard deviation hypothesis test to check whether the range sample point for each aircraft type can be assumed constant.

Step 3 Compute the range (ground distance) travelled during climb, R_{climb}. We assume the climb segment to start from the 0 altitude and end at cruise altitude as shown in Figure 4. We use 10 samples of different total payload for each aircraft type to obtain the climb range by running BADA trajectory simulations. From these simulation data we derive the regression model for climb range for each aircraft type with total payload as the input variable. Before we can compute the climb fuel burn, we first need to find the aircraft weight at the end of the climb segment, which we can easily obtain once we compute the cruise fuel burn.

Step 4 Compute $W_{\text{f, descent}}$, by assuming that the amount of fuel burned during descent is equal to fuel burned during cruise for the same flight range ($\tilde{W}_{\text{f, cruise}}$) minus the descent fuel factor as:

$$W_{\text{f, descent}} = \tilde{W}^{\text{eq}}_{\text{f, cruise}} - f_{\text{WL}} W_{\text{L}} - f_{\text{R}} R + \text{C}. \tag{5}$$

$\tilde{W}^{\text{eq}}_{\text{f, cruise}}$ is obtained using the Breguet range equation, where W_i and W_f correspond to W_1 and W_{ZF} (refer to Figure 4), respectively. The correction factors, f_{WL}, f_{R}, and C are derived based on BADA results. The mission parameters, W_{L} and R, refer to the landing weight and segment range, respectively.

Step 5 Compute the fuel burn during cruise segment, W_{cruise}, as follows:

$$W_{\text{cruise}} = W_0 - W_1, \tag{6}$$

where W_0 and W_1 are the initial and final weight of the cruise segment, as shown in Figure 4. The cruise final weight can be obtained by adding the previously computed $W_{\text{f, descent}}$ to the zero-fuel weight (which includes the payload). W_0 can be found by implementing the Breguet range equation (Eqn. 1), by first obtaining the cruise range, R_{cruise}:

$$R_{\text{cruise}} = R_{\text{total}} - R_{\text{climb}} - R_{\text{descent}} - R_{\text{takeoff}} - R_{\text{landing}}. \tag{7}$$

The R_{climb} and R_{descent} have been obtained from the previous step. The distance required for takeoff, R_{takeoff}, and for landing, R_{landing} are obtained from the SKYbrary website[7]. We assume that R_{takeoff} and R_{landing} are constant for each aircraft type. Once W_0 is known, we can obtain the fuel burn by using Equation 6.

Step 6 Compute the fuel burn during the climb segment, W_{climb}, by implementing the fuel increment factor f_{climb}:

$$W_{\text{f, climb}} = \frac{\tilde{W}^{\text{eq}}_{\text{f, cruise}} + f_{\text{climb}} W_0}{(1 - f_{\text{climb}})}, \tag{8}$$

where W_0 refers to final weight of the climb segment as illustrated in Figure 4. This weight can be obtained by rearranging Eqn. 6 into $W_0 = W_{\text{cruise}} + W_1$, where the W_{cruise} was obtained from the previous step. The final and initial weights on $\tilde{W}_{\text{f, cruise}}$ are referred to the weights on the climb segment. The formula above is the same as the one used by Lee and Chatterji (Lee and Chatterji, 2010); however, we derive the fuel factor from BADA simulation results. The fuel factor is assumed constant for each aircraft type.

Step 7 Compute the maneuver fuel burns by using the *fuel factor*, following the approach by Lee and Chatterji (Lee and Chatterji, 2010), and using their recommended values as well. The fuel increment factor is used as a fraction of weights. The maneuver fuel weight, $W_{\text{f, man}}$, is typically expressed as a fixed fraction of the takeoff weight (W_{TO}), which can be obtained by substituting the result from Eqn. 8 to $W_{\text{TO}} = W_{\text{f, climb}} + W_0$, with f_{man} set to 0.007 (Kroo, Sept 2006). This relation is expressed below,

$$W_{\text{f, man}} = W_{\text{TO}} \cdot f_{\text{man}} \tag{9}$$

Upon completing the above procedure, we obtain the fuel burn value corresponding to a flight mission. Once we run this procedure with all flight missions in the inventory, we obtain a fuel burn database.

[7] http://www.skybrary.aero/index.php/Category:Aircraft

Table 3: Flight mission simulation for A320 with total distance 2 655.768 km and payload 15 562.5 kg.

Input		**Model**	**Output**
Step 1: *Calculate reserve fuel as additional payload*			
P_{int}	$\rightarrow 15\,562.5$ kg	$W_{\text{ZF}} = \text{OEW} + P_{\text{int}}$	
OEW	$\rightarrow 37\,500$ kg		
W_{ZF}	$\rightarrow 53\,062.5$ kg	$W_{\text{f, res}} = W_{\text{ZF}} \cdot f_{\text{res}}$	$W_{\text{f, res}} \rightarrow 4\,425$kg
f_{res}	$\rightarrow 0.08$		(additional payload)
Step 2: *Calculate the descent range*			
		$P = P_{\text{int}} + W_{\text{f, res}}$	
P	$\rightarrow 19\,987.5$ kg	Constant range	$R_{\text{descent}} \rightarrow 207.575$ km
Step 3: *Calculate the climb and cruise range*			
P	$\rightarrow 19\,987.5$ kg	$R_{\text{climb}} = 0.005P + 109.4$	$R_{\text{climb}} \rightarrow 209.13$ km
R_{total}	$\rightarrow 2\,655.768$ km		
R_{takeoff}	$\rightarrow 2\,190$ m	$\sum R_{\text{other}} = R_{\text{climb}} + R_{\text{descent}} + R_{\text{takeoff}} + R_{\text{landing}}$	
R_{landing}	$\rightarrow 2\,190$ m	$R_{\text{cruise}} = R_{\text{total}} - \sum R_{\text{other}}$	$R_{\text{cruise}} \rightarrow 2\,235.43$ km
Step 4: *Calculate descent fuel*			
		$W_{\text{L}} = W_{\text{ZF}} + P$	
W_{L}	$\rightarrow 57\,487.5$ kg	$\Delta W = 0.023W_{\text{L}} + 2.63R - 1\,410.35$	
R_{descent}	$\rightarrow 207.575$ km	$W_{\text{f, descent}} = \tilde{W}^{\text{eq}}_{\text{f, cruise}} - \Delta W$	$W_{\text{f, descent}} \rightarrow 315.997$ kg
Step 5: *Calculate cruise fuel*			
		$W_1 = W_{\text{f, descent}} + W_{\text{L}}$	
W_1	$\rightarrow 57\,803.5$ kg		
V	$\rightarrow 833.4$ km/h		
c_T	$\rightarrow 0.573$ N/(N $\cdot$ h)	$R = \frac{V}{c_T}\frac{L}{D}\ln\left(\frac{W_0}{W_1}\right)$	
L/D	$\rightarrow 18.5$		
R_{cruise}	$\rightarrow 2\,235.43$ km	$W_{\text{f, cruise}} = W_0 - W_1$	$W_{\text{f, cruise}} \rightarrow 4\,992.03$ kg
Step 6: *Calculate climb fuel*			
		$W_0 = W_{\text{f, cruise}} + W_1$	
W_0	$\rightarrow 62\,795.53$ kg	$W_{\text{f, climb}} = \frac{\tilde{W}^{\text{eq}}_{\text{f, cruise}} + 0.0166W_0}{(1-0.0166)}$	$W_{\text{f, climb}} \rightarrow 1\,553.795$ kg
Step 7: *Calculate maneuver fuel*			
		$W_{\text{TO}} = W_{\text{f, climb}} + W_0$	
W_{TO}	$\rightarrow 64\,349.32$ kg	$W_{\text{f, man}} = W_{\text{TO}} \cdot 0.007$	$W_{\text{f, man}} \rightarrow 449.185$ kg
Calculate total fuel			
$W_{\text{f}} = W_{\text{f, descent}} + W_{\text{f, cruise}} + W_{\text{f, climb}} + W_{\text{f, man}} \rightarrow 7\,311.007$ kg			

Table 3 shows an example of the segment-by-segment computation, performed for an A320 aircraft with flight mission distance $2\,655.768$ km and payload $15\,562.5$ kg. This selected flight mission falls in the long-haul mission flight category. In this example, the step-by-step procedure following the flowchart in Figure 8 is listed in detail. The aircraft parameters listed in Table 2 are used for this computation.

The developed medium-fidelity segment-by-segment model also offers computational time efficiency, as shown in Table 4. This table also includes the computational time of two high-fidelity models, one low-fidelity model. We show the computational time required to compute the fuel burn for one complete flight mission. Note that there are computational time variations even when the same method is used, depending on the flight mission to be solved. Among the methods shown here, only the surrogate-based mission analysis model (Liem et al., 2015b) was performed in parallel, with 16 processors. The computations for the BADA trajectory simulation and ICAO Calculator are done via the online platform, which adds to the computational time overhead. The proposed medium-fidelity approach shows a clear advantage in terms of computational time, which requires less than 8.8 microseconds to complete one flight mission.

Table 4: Computational time comparison between several fuel burn models.

Model	**Specification**	**Required time (1 mission)**
High-fidelity (Liem *et al.* (Liem et al., 2015b))	16 processors	6–18 minutes
High-fidelity (BADA)	Online ($\sim$ 90 Mbps)	1–2 minutes
Low-fidelity (ICAO Calculator)	Online ($\sim$ 90 Mbps)	20–40 seconds
Proposed approach		
Medium-fidelity	1 processors	7.8–8.8 microseconds

Figure 10 shows the distribution of total fuel burn for different mission range (in the x-axis) and mission payload (indicated by the colormap). Only three representative aircraft types (Boeing 777-200ER, Airbus 320-100, and McDonnell Douglas DC9 Super80) are shown here, due to the space constraint. However, similar trends are observed on all other 37 remaining aircraft types. These fuel burn inventories will be used as the sample data to derive fuel burn linear regression models, which area discussed next.

3.4. Regression model

A regression model to approximate fuel burn is derived for each aircraft type. As previously mentioned, we employ two-dimensional linear regression models, with mission payload P and range R as inputs, and

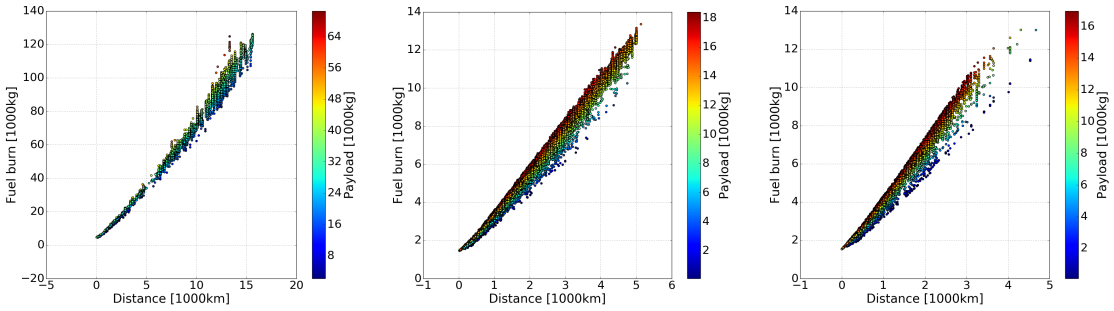

(a) Boeing 777-200ER (b) Airbus 320-100 (c) McDonnell Douglas DC9

Figure 10: Fuel burn plots as functions of mission range and payload for three sample aircraft types.

fuel burn as output. This equation is expressed as follows:

$$W_{\mathrm{f},ij} = \alpha_j R_{ij} + \beta_j P_{ij} + \gamma_j + \epsilon_{ij}, \tag{10}$$

where i denotes the flight index within an aircraft type and j denotes the aircraft type index. The variables α_j, β_j, and γ_j are the regression parameters for the aircraft type j, and W_{f} refers to the fuel burn. ϵ_{ij} is the error term for a specific flight, i.e., the discrepancy between the linear approximation of fuel burn $\tilde{W}_{\mathrm{f},ij}$ and the actual fuel burn $W_{\mathrm{f},ij}$. This error has a normal distribution with a mean 0 and a variance σ^2, i.e., $\epsilon \sim \mathcal{N}\left(0, \sigma^2\right)$. The method of least squares is employed to derive α_j, β_j, and γ_j. The selected regression parameters for a specific aircraft type are denoted as a_j, b_j, and c_j. Thus the approximation model can be expressed as:

$$\tilde{W}_{\mathrm{f},ij} = a_j R_{ij} + b_j P_{ij} + c_j \tag{11}$$

Once the fuel burn model is derived and these parameters are obtained, we can easily find the approximated total fuel burn for each aircraft type by simply:

$$\mathbf{W}_{\mathrm{f},j} = a_j \sum_{i=1}^{N_{f\,j}} R_{ij} + b_j \sum_{i=1}^{N_{f\,j}} P_{ij} + N_{f\,j} \cdot c_j, \tag{12}$$

where $N_{f\,j}$ is the total number of flight missions. Equation (12) offers a significant computational cost reduction in estimating the total aggregate fuel burn, as the fuel burn computation for each flight is no longer required. The prediction error of this summation will have a mean value of 0, which is derived in the following expression:

$$\mathbb{E}\left[\mathbf{W}_{\mathrm{f},j}\right] = \mathbb{E}\left[N_{f\,j}\epsilon_j\right] = N_{f\,j} \cdot \mathbb{E}\left[\epsilon_j\right] = 0, \tag{13}$$

since we know that $\mathbb{E}[\epsilon_j] = 0$.

The *goodness of fit* of the derived linear regression functions is evaluated by computing the *coefficient of determination*, or R^2. This accuracy measure indicates how well the regression line approximates the real data points. R^2 values range from 0 to 1; when $R^2 = 1$ the regression line fits the data perfectly. The derived coefficients could also provide insight into how much a change in each input variable would affect the total fuel burn computation. Table 5 lists the derived linear regression equation. The corresponding R^2 values for each aircraft are also displayed including the number of flight missions that are used as samples. We can observe that all R^2 values are greater than 0.99, which tells us that the linear relationship assumption is still valid even though it is not perfectly linear as shown in Figure 10, and that the total fuel burn can be sufficiently explained by the selected two input variables. The hundreds or thousands of flight missions considered for each aircraft type has distinct mission specifications, and yet the generated fuel burn data show that there is a "pattern" within each aircraft type. From the regression coefficients shown in Table 5, we can see that the flight's fuel burn depends largely on the mission range, and much less so on the mission payload.

The model derivation and validation are performed with two separate data sets. The derived regression fuel burn model is validated using the 2016 data obtained from the BTS. The error between the fuel burn computed using the segment-by-segment fuel burn computation procedure and the derived regression model is quantified using the root mean square deviation (RMSD). We perform two types of validation to evaluate the error. The first is to validate the accuracy of the prediction *for each flight mission data*, i.e., for each data point. This validation is performed using 10 sets of 100 randomly selected samples and will be denoted as the "individual-sampling" validation. The percentage error is then calculated using the average RMSD from all repetitions, and the standard error is computed from the standard deviation corresponding to each repetition. Secondly, we calculate the RMSD of the aggregate fuel burn computation using the same samples as the individual-sampling validation, denoted as the "aggregate" validation. For this purpose, we take the summation of all computed fuel burn corresponding to each aircraft type from each set. We then obtain the difference between the total aggregate fuel burn computed after performing the fuel burn for each flight mission one-by-one, and by applying Equation (12).

Figure 11 shows the percentage error (RMSD) for both conditions and the corresponding standard error for individual sampling conditions for all aircraft types considered in this study. We observe from Figure 11 that the percentage error (RMSD) for the individual sampling validation is at least one order of magnitude higher than that of the aggregate validation. The maximum values for those are around 9.08% and 0.83%,

Table 5: The list of aircraft type, the number of flight missions included to generate the fuel burn database, and the derived two-dimensional linear regression model for each aircraft type.

No.	Aircraft Name	No. of Flights	Regression Model	R^2
1	Airbus Industrie A-318	123	$W_f = 1.632R + 0.115P + 489.412$	0.998
2	Airbus Industrie A319	24 113	$W_f = 2.059R + 0.088P + 164.974$	0.996
3	Airbus Industrie A320-100/200	29 175	$W_f = 2.256R + 0.071P + 161.171$	0.997
4	Airbus Industrie A321	4 767	$W_f = 2.900R + 0.110P - 280.856$	0.997
5	Airbus Industrie 330-200	4 005	$W_f = 9.301R + 0.270P - 8691.448$	0.996
6	Airbus A330-300	1 327	$W_f = 9.184R + 0.227P - 5520.892$	0.997
7	Airbus Industrie A340-200	506	$W_f = 9.006R + 0.304P - 11768.010$	0.995
8	Airbus Industrie A340-300	372	$W_f = 9.683R + 0.309P - 12865.092$	0.996
9	Airbus Industrie A340-500	146	$W_f = 12.10R + 0.401P - 20570.166$	0.996
10	Airbus Industrie A340-600	465	$W_f = 13.75R + 0.319P - 21224.290$	0.994
11	Boeing 737-100/200	341	$W_f = 2.411R + 0.100P + 408.615$	0.996
12	Boeing 737-300	11 243	$W_f = 2.375R + 0.089P + 31.551$	0.997
13	Boeing 737-400	5 403	$W_f = 2.709R + 0.107P - 31.517$	0.990
14	Boeing 737-500	790	$W_f = 2.087R + 0.062P + 510.817$	0.997
15	Boeing 737-600	224	$W_f = 2.187R + 0.134P - 200.716$	0.998
16	Boeing 737-700/700LR	26 228	$W_f = 2.311R + 0.104P - 177.694$	0.996
17	Boeing 737-800	33 809	$W_f = 2.865R + 0.101P - 307.557$	0.996
18	Boeing 737-900	10 171	$W_f = 2.784R + 0.112P - 518.667$	0.997
19	Boeing 737-900ER	821	$W_f = 2.839R + 0.110P - 519.074$	0.997
20	Boeing 747-200/300	129	$W_f = 11.89R + 0.320P - 18013.410$	0.998
21	Boeing 747-400	1 789	$W_f = 10.78R + 0.188P - 9875.112$	0.994
22	Boeing 747-800	148	$W_f = 5.154R + 0.133P - 527.531$	0.998
23	Boeing 757-200	10 256	$W_f = 3.382R + 0.116P - 367.634$	0.997
24	Boeing 757-300	1 857	$W_f = 3.626R + 0.098P - 123.242$	0.997
25	Boeing 767-200/ER/EM	315	$W_f = 4.655R + 0.183P - 1372.803$	0.995
26	Boeing 767-300/300/300ER	6455	$W_f = 5.845R + 0.233P - 4641.441$	0.993
27	Boeing 777-200ER/200LR/233LR	4 732	$W_f = 7.578R + 0.364P - 13028.213$	0.992
28	Boeing 777-300/300ER/333ER	1 791	$W_f = 9.137R + 0.322P - 16019.100$	0.994
29	Boeing 787-800 Dreamliner	1 450	$W_f = 2.086R + 0.144P - 359.991$	0.997
30	Boeing 787-900 Dreamliner	376	$W_f = 2.238R + 0.140P - 410.398$	0.997
31	Canadair RJ-100/RJ-100ER	185	$W_f = 0.891R + 0.091P + 260.154$	0.999
32	Canadair RJ-200ER /RJ-440	20 641	$W_f = 0.994R + 0.065P + 293.568$	0.996
33	Canadair RJ-700	18 455	$W_f = 1.260R + 0.080P + 363.714$	0.996
34	Canadair CRJ 900	14 586	$W_f = 1.338R + 0.075P + 350.152$	0.997
35	Embraer-140	2645	$W_f = 0.736R + 0.065P + 297.519$	0.998
36	Embraer-145	17 974	$W_f = 0.769R + 0.067P + 263.242$	0.997
37	Embraer 170	7 644	$W_f = 1.313R + 0.078P + 216.084$	0.998
38	Embraer 190	5 756	$W_f = 1.763R + 0.075P + 388.843$	0.997
39	McDonnell Douglas DC9 Super 80/MD81/82/83/88	13 976	$W_f = 2.762R + 0.094P + 116.153$	0.995
40	McDonnell Douglas MD-90	2 619	$W_f = 2.419R + 0.058P + 595.476$	0.998

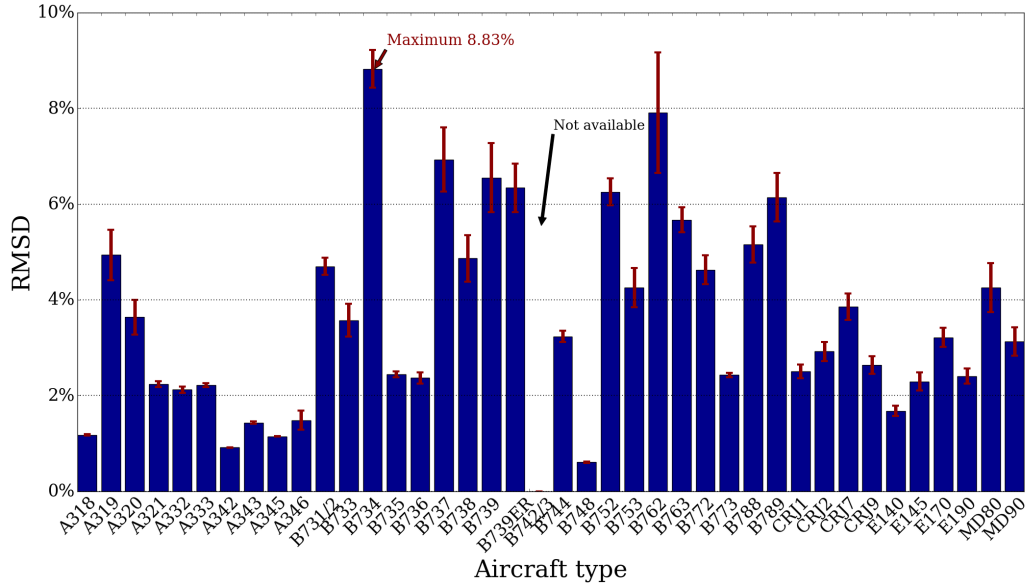

(a) RMSD for individual sampling

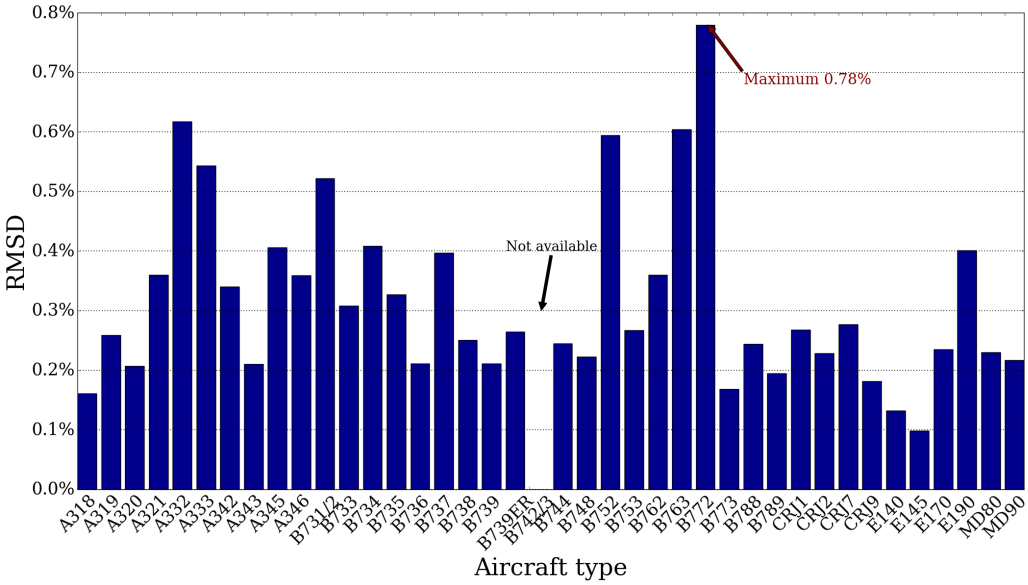

(b) RMSD for aggregate

Figure 11: Percentage error between regression fuel burn model and fuel burn computation.

respectively. This result is not surprising, and is consistent with the predicted expected aggregate error as shown in Equation 13. From this result, we can confidently use the derived regression model to accurately estimate the total fuel burn corresponding to an aircraft type, thereby significantly reducing the computational cost.

After validating the regression model with a different set of database, we also perform the validation with actual fuel burn from the airlines' report. The actual fuel burn information is obtained from the same source as the flight mission database, which is the BTS Air Carrier Financial : Schedule P-12(a) [8]. In this validation, we use the aggregate actual fuel burn of the United Airlines, JetBlue Airways, and Virgin America Airlines for each month, since the breakdown of mission-by-mission fuel burn is not publicly available. The number of evaluated flight mission for these airlines is listed in Table 6, including the aircraft types for each corresponding airliner. Figure 12 shows the percentage error between the actual aggregate fuel burn and the fuel burn computed using the derived regression model for each month. Solid blue line with filled-circle markers indicates the percentage error with fuel burn from the year 2015 and the dashed red line with filled-triangle markers indicate the percentage error with fuel burn from the year 2016. The fuel burn from the regression model is computed by taking the flight missions for each airliner corresponding to the aircraft type, month and year.

The errors shown in the comparison with the actual airlines' data include the operational variations that are not yet properly modeled in our current approach. For instance, we have not yet taken into account the variation of weather conditions (which might cause flight reroute or detour), taxi-in and taxi-out time that depend on the surface routes. Moreover, we only use the predicted payload for each flight mission, which might differ from the actual payload carried by the aircraft. However, these results are encouraging since the maximum percentage error is less than 6%. Moreover, this model also gives an additional computational benefit (compared to that presented in Table 4) since the total aggregate fuel burn can be computed without computing the fuel burn one by one. For instance, this model only requires 0.0031 seconds to evaluate the aggregate fuel burn for Airbus A320 ($29\,175$ missions). When we use the segment-by-segment medium-fidelity approach, we need 0.33 seconds to evaluate that many flight missions. We can therefore use this inexpensive model to predict the total fuel burn quite accurately and to perform the uncertainty quantifica-

[8] Bureau of Transportation Statistic (BTS), "Database Name: Air Carrier Financial: Schedule P-12(a)." US Department of Transportation. https://www.transtats.bts.gov/DL_SelectFields.asp?Table_ID=294&DB_Short_Name=Air%20Carrier%20Financial

Table 6: The number of departures and the aircraft types for United Airlines, JetBlue Airways, and Virgin America Airlines in year of 2015-2016.

Aircraft type	**Flight mission**	
	2015	**2016**
United Airlines		
Boeing 737-700/700LR	40 452	43 676
Boeing 737-800	145 266	145 995
Boeing 757-200	46 007	40 602
Boeing 757-300	16 004	17 501
Boeing 767-300/300ER	16 549	16 307
Boeing 777-200ER/200LR/233LR	33 063	36 469
Boeing 737-900	157 611	175 361
Airbus Industrie A320-100/200	118 943	122 539
Airbus Industrie A319	70 677	73 158
Boeing 747-400	7 458	6 502
Boeing 787-800 Dreamliner	6 320	6 028
Boeing 787-900 Dreamliner	3 180	7 097
JetBlue Airways		
Embraer 190	114 581	117 073
Airbus Industrie A320-100/200	181 845	187 445
Airbus Industrie A321	17 477	32 670
Virgin America Airlines		
Airbus Industrie A319	48 775	57 800
Airbus industrie A320-100/200	13 413	12 085

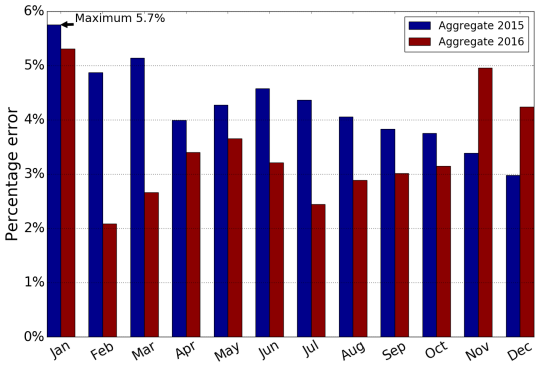

(a) United Airlines

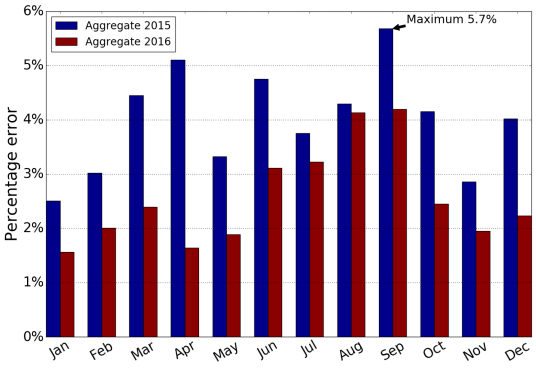

(b) JetBlue Airways

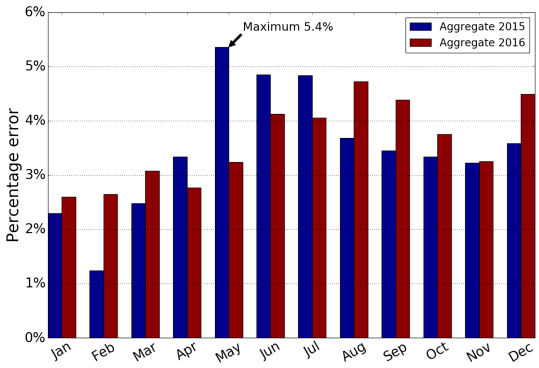

(c) Virgin America Airlines

Figure 12: Percentage error between regression fuel burn model and actual fuel burn from airlines.

tion efficiently, especially when the total aggregate fuel burn computation is required. Rojo, for instance, performed the uncertainty analysis to compute the variance of the difference in aviation-induced local air quality impacts between baseline and policy (Rojo, 2007). The Monte Carlo simulation technique will also be useful to perform global sensitivity analysis (GSA), to provide the importance ranking of input factors based on their significance (Saltelli et al., 2008). The GSA results can guide channelling research efforts to reduce model output uncertainty (Allaire, 2009). Liem demonstrated the use of the GSA technique to find the key input drivers in the aviation impact on air quality, in the context of technology infusion policy analysis (Liem, 2010). In this case, the technology infusion policy refers to the introduction of new technology aircraft as part of the efforts to mitigate the environmental impact of aviation. These uncertainty and sensitivity analysis studies, however, are beyond the scope of the current paper.

4. Fuel burn performance study

In this section, we investigate two common assumptions in fuel burn modeling, namely the cruise-only approximation and the similar aircraft type mapping when no appropriate database is available. To perform these studies, we use the derived fuel burn prediction model described in Section 3.3.

4.1. Cruise-only approximation study

It is common to use the cruise fuel burn as a surrogate for the entire flight mission's fuel burn (Liem et al., 2015a) as the cruise segment is often considered as the most significant flight segment. This assumption is typically used to simplify the mission profile and thus the fuel burn computation, at the expense of accuracy. We aim to investigate the fuel burn prediction error associated with this assumption. The error comparison will be done for each aircraft type. Figure 13 illustrates the difference between the standard mission profile (as previously shown in Figure 4) and the cruise-only approximation for the same flight mission range. For the cruise-only approximation, the climb and descent segments are not modeled and the entire mission range becomes the cruise range.

To conduct the study, we recompute the fuel burn for each flight mission by assuming the cruise-only mission profile, by following the procedure presented in Step 5 of Section 3.3. The computed fuel burn is then compared to the one previously obtained via the segment-by-segment fuel burn computation (excluding the reserve and maneuver fuels). This comparison is performed for each flight mission. To quantify the discrepancies, we compute the corresponding percentage (RMSD) errors. Figure 14 shows the RMSD for all aircraft types using the available BTS mission data from the years of 2015 (blue) and 2016 (red). The

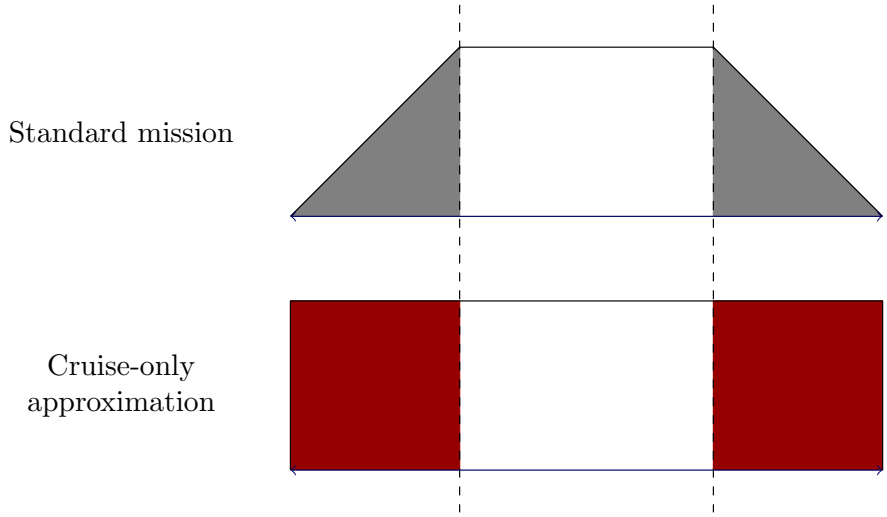

Figure 13: Comparison between standard and cruise-only assumption mission profile.

aircraft types are ordered based on their empty weight, to reflect their sizes. The leftmost (E145) is the smallest aircraft type, and the rightmost (A346) is the largest. Note that some aircraft types did not operate in 2016 thus they are omitted in the plot. The discrepancies range from 4.3% to 45%, and we observe a general trend that the cruise-only approximation is closer to the segment-by-segment computation for larger aircraft. The smaller aircraft typically fly shorter ranges, and encounter the largest errors. Conversely, the larger aircraft mostly fly longer ranges, resulting in smaller errors associated with the cruise-only approximation. Indeed the trend is not strictly consistent; however, note that the empty weight is only an approximate proxy for the aircraft size, and that some aircraft types fly a wide range of flight distances. Depending on the flight distance distribution within each aircraft type, the RMSD might vary and deviate from the general trend.

The cruise-only approximation, which does not reflect the actual aircraft operation and yet is often adopted in fuel burn estimation, can therefore lead to large errors. These errors can propagate to any subsequent analyses. This is undesirable and further emphasizes the importance of making the more realistic assumption in the modeling process.

4.2. Similar aircraft type mapping

Most fuel burn models are derived based on empirical data, which imposes challenges when we evaluate a new aircraft variant or when the data are not available or outdated. This phenomenon is quite common

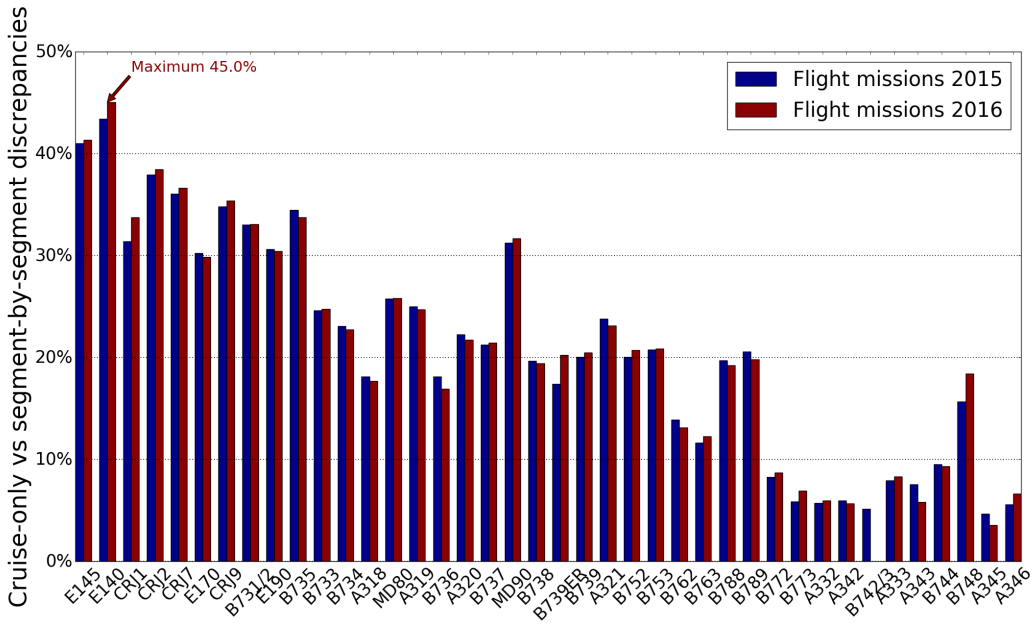

Figure 14: Fuel burn RMSD between the cruise-only approximation and segment-by-segment computation for all aircraft types. The aircraft types are ordered based on the empty weight, from the smallest (E145) to largest (A346). We can observe a general trend that the discrepancy decreases as the aircraft gets larger, as the corresponding flight ranges are longer.

when using fuel burn database (e.g., SAGE) (Wasiuk et al., 2015). Here we investigate the errors associated with such a mapping. Instead of manually identifying similar aircraft types, we employ a systematic machine learning method to group similar aircraft types together. Once the groups are identified, we derive cluster regression functions to compute the fuel burn of the cluster member. These new fuel burn values represent the values obtained when no appropriate data are available. The discrepancies between these values and those computed with the appropriate fuel burn models highlight the errors associated with the similar aircraft type mapping.

Since we want to discover groups of similar characteristics within a pool of unlabeled data by finding the data's hidden structure, an *unsupervised learning algorithm* is used for this purpose. In particular, we employ the classical K-means clustering algorithm (Steinhaus, 1956; Lloyd, 1982; MacQueen, 1967). We use the gradient information from the derived regression models, $\partial W_{\mathrm{f}}/\partial R$ and $\partial W_{\mathrm{f}}/\partial P$, as inputs to the unsupervised clustering algorithm. These quantities reflect the fuel burn performance of each aircraft type, by indicating how much, on average, a unit change in mission range and payload affects the amount of fuel burned. By doing so, we can group aircraft types with similar fuel burn performance together.

We first divide the aircraft types into three clusters. The clustering results show that the algorithm can automatically group aircraft types with similar sizes together as shown in Figure 15. Each symbol represents a different aircraft type. Cluster 1 members are represented with black filled-triangle markers, cluster 2 members are represented with blue filled-diamond markers, and cluster 3 members are represented with red filled-circle markers. These clusters group aircraft types with seat capacity more than 300 (e.g., Airbus A330, Airbus A340, Boeing B747, Boeing B777), those with seat capacity between 200 and 300 (e.g., Boeing 757, Boeing 767), and those with seat capacity less than 200 (e.g., Airbus A320, Boeing 737, Embraer and Canadair regional aircraft). While this might seem straightforward in this simple case, the automatic clustering will help significantly when we deal with a larger set of data, especially when we also consider the engine variation within each aircraft type.

From this result, we derived a regression model for each cluster by randomly taking 70% of the flight missions within each cluster. These newly derived regression models would subsequently be referred to as the *cluster regression model*, to differentiate it from the individual aircraft type's regression model. We observe that payload variable is only affected within the aircraft type and the cluster regression models lose the dependency to on payload, therefore, the cluster regression model is derived with mission range as an input variable. R^2 for these regression models is calculated as shown in Table 7.

We validate the regression model corresponding to each cluster with the 2016 BTS flight mission database.

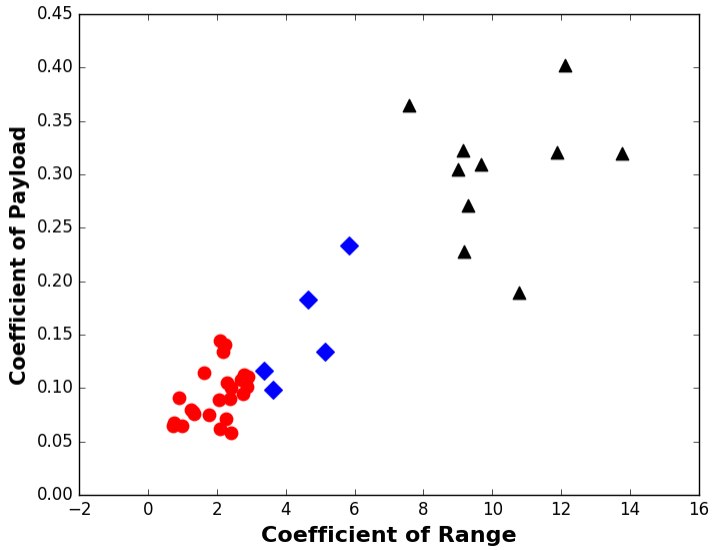

Figure 15: Clustering results using the K-means clustering algorithm, using the gradients of fuel burn with respect to distance and payload as the clustering criterion.

To perform the validation, we first compute the total aggregate fuel burn for each aircraft type using the cluster regression model, depending on which cluster the aircraft type belongs to. The aggregate fuel burn error is then computed by comparing this value with the total aggregate fuel burn obtained using the segment-by-segment fuel computation corresponding to that particular aircraft type. The RMSD for each cluster is then computed from these errors, which is shown in Figure 16. We can see from these results that the similar aircraft type mapping encounters high errors, with 12.69% being the minimum error among the three clusters. Compared to the individual total aggregate fuel burn errors shown in Figure 11, these errors are significantly higher.

The high error levels might be due to the many aircraft types included in one cluster, i.e., the characteristic variation that needs to be modeled within each cluster. Cluster 3, for instance, contains 25 aircraft types. To investigate further, we further refine the clustering by performing another level of clustering within each cluster, employing the same algorithm. The resulting new clusters are referred to as *sub-cluster*. This second-level clustering is only performed on clusters 1 and 3, since cluster 2 only has 5 members. Clusters 1 and 3 will have 4 sub-clusters each, therefore cluster 2 will become sub-cluster 5. The updated sub-cluster regression models and R^2 are listed in Table 8.

Table 7: Aircraft type distribution with K-means clustering including the linear regression model for each cluster.

Cluster	Aircraft type	Regression Model	$\mathbf{R^2}$
1	Airbus Industrie A330 Family Airbus Industrie A340 Family Boeing 747-200/300 Boeing 747-400 Boeing 777 Family	$W_{\mathrm{f}} = 8.436R + 2460.982$	0.849
2	Boeing B747-8 Boeing 757 Family Boeing 767 Family	$W_{\mathrm{f}} = 5.542R - 2388.964$	0.902
3	Airbus A318 Airbus A319 Airbus A320-100/200 Airbus A321 Boeing 737 Family Boeing 787 Family Canadair RJ Family Embraer Family McDonnell Douglas Family	$W_{\mathrm{f}} = 2.669R + 221.947$	0.895

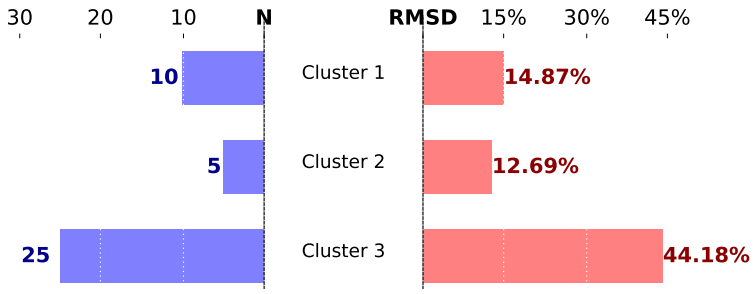

Figure 16: Number of aircraft type within the cluster (left side) and RMSD for the total aggregate fuel burn computation error (right side) for each cluster.

Table 8: Aircraft type distribution with K-means sub-clustering including the regression model for each cluster.

Sub-Cluster	**Aircraft type**	**Regression Model**	$\mathbf{R^2}$
1	Boeing 777-200ER/200LR/233LR	$W_{\mathrm{f}} = 7.735R - 3615.513$	0.985
2	Airbus Industrie A330 Family Airbus Industrie A340-200 Airbus Industrie A340-300 Boeing 777-300/300ER/333ER	$W_{\mathrm{f}} = 8.929R + 286.908$	0.985
3	Airbus Industrie A340-500 Airbus Industrie A340-600 Boeing 747-200/300	$W_{\mathrm{f}} = 13.126R - 10460.714$	0.944
4	Boeing 747-400	$W_{\mathrm{f}} = 10.825R - 3160.681$	0.991
5	Boeing 747-800 Boeing 757 Family Boeing 767 Family	$W_{\mathrm{f}} = 5.577R - 2497.433$	0.916
6	Airbus Industrie A319 Airbus Industrie A320-100/200 Boeing 737-100/200 Boeing 737-300 Boeing 737-500 Boeing 737-600 Boeing 737-700/700LR Boeing 787 Family McDonnell Douglas MD-90	$W_{\mathrm{f}} = 2.301R + 973.519$	0.986
7	Airbus Industrie A321 Boeing 737-400 Boeing 737-800 Boeing 737-900 Boeing 737-900ER McDonnell Douglas DC9 - Super 80/MD81/82/83/88	$W_{\mathrm{f}} = 2.886R + 1033.031$	0.985
8	Airbus Industrie A318 Embraer 190	$W_{\mathrm{f}} = 1.757R + 986.132$	0.987
9	Canadair RJ Family Embraer 140 Embraer 145 Embraer 170	$W_{\mathrm{f}} = 1.283R + 500.238$	0.801

Figure 17 shows the updated RMSD. The clustering algorithm results in a single aircraft type in some cases (clusters 1 and 4), and thus their corresponding errors are the same as those shown in Figure 11. From these results we can observe that the errors are reduced after performing the sub-clustering. However, there error are still considered as large with maximum error around 22.726% compared to error of total aggregate fuel burn for each aircraft type. Based on the above observation, we can see that each aircraft type has a unique "characteristic" in terms of fuel burn performance. Even with systematic mapping, the corresponding fuel burn prediction error could be quite significant, which might affect any subsequent analysis and decision makings considerably. Therefore, care must be taken when we use other aircraft type's data to predict fuel burn. We need to be aware of the prediction error, and take that into consideration when analyzing the results. Ideally, we need to use a specific fuel burn prediction model for each aircraft type, which truly reflects its actual fuel burn performance. The clustering errors might be different once we refine the fuel burn models. For instance, we might obtain more accurate clustering by including engine parameters in the regression models. This, however, is beyond the scope of the current paper but will be considered for future work.

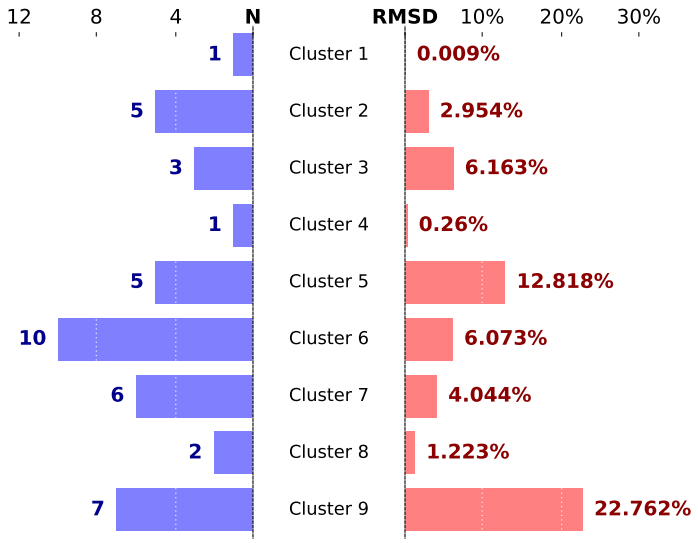

Figure 17: Number of aircraft type within the sub-cluster (left side) and RMSD for the total aggregate fuel burn computation error (right side) for each sub-cluster, after performing a second-level of clustering within clusters 1 and 3.

5. Conclusion

In this paper, we have developed a data-enhanced medium-fidelity modeling technique that can significantly reduce the computational cost required to compute the total aggregate fuel burn. In particular, we reduced the computational cost by $\mathcal{O}\left(10^4\right)$, i.e., from the total number of flight missions ($\mathcal{O}\left(10^5\right)$) to the number of aircraft types ($\mathcal{O}\left(10\right)$). A linear regression model was derived for each aircraft type, which relied on fuel burn database corresponding to actual aircraft operation data in a year, where the flight data were obtained from the BTS database. The linear regression model took payload and range as inputs. The fuel burn database was generated using the developed medium-fidelity fuel burn computation model, which was derived based on the Breguet range equation and BADA simulation results data. With the data integration, we derived a model that was accurate to the BADA fuel burn simulation model. Moreover, this approach was more computationally efficient, since we did not need to run the simulation for each flight mission's segment. The developed models were validated using a flight mission database from another year of operation, also from BTS. The results showed that the linear regression model could predict the total aggregate fuel burn with less than 1% approximation error. When compared with actual fuel burn from 3 different airlines (United Airlines, Jetblue Airways, and Virgin America Airlines), the errors were less than 6%. Moreover, the linear regression model could offer a speedup of approximately 100 times compared to the segment-by-segment medium-fidelity approach. These results showed that the models were both efficient and accurate, and thus can be used with confidence in any subsequent decision-making and policy analysis.

We used the derived models to investigate two common simplifications and assumptions in fuel burn modeling, namely the cruise-only assumption and the similar aircraft type mapping. The cruise-only assumption ignored the climb and descent segments in the mission profiles; however, our study showed that this simplification would not give an accurate fuel burn computation results, especially for smaller aircraft. Larger aircraft mostly flew longer distances, which made the cruise segment more dominant in the flight mission profile. Correspondingly, the errors associated with the cruise-only approximation were smaller. This inaccuracy would lead to undesirable results should we use them in any subsequent analysis or as bases for decision making. These results highlighted the need to consider the different segments in the flight mission profile, and to model them separately. Using the approach proposed in this paper, we can perform the segment-by-segment fuel burn computation to achieve a good accuracy without any significant added computational burden. The similar aircraft type mapping was commonly used when the reference data pertaining to a specific aircraft type was unavailable in the database of model, e.g., BADA. This typically involved newer aircraft variants or the less commonly used aircraft. To emulate this mapping, we employed

an unsupervised learning (K-means clustering) algorithm, based on the fuel burn performance reflected in the linear regression coefficients derived earlier. Upon performing two-level clustering procedures, and deriving a cluster regression model for each cluster, we achieved prediction accuracies ranging between 1.22% and 22.76%. These results attested that each aircraft type had a unique fuel burn performance, and thus using data corresponding to other aircraft types in the fuel burn approximation might result in significant computation errors.

Due to the data-based nature of the proposed approach, the effectiveness of the derived models was limited by the operational range within which the models were derived. In particular, this work focuses on the US market, which might not be representative to other operational regions. To expand the database, more aircraft types and operational regions should be considered in the model derivation to represent the actual aircraft-type distribution in the current global air transportation system. Likewise, further investigations would be required to enable modeling future technology, since the derivations still rely on past data. By using the same approach, the BADA simulation results could be replaced by other high-fidelity models. For instance, we could use a more detailed aircraft performance model that modeled a new technology (e.g., a new engine or aircraft design) as the high-fidelity model. The medium-fidelity modeling approach would still apply, even with different low- and high-fidelity models. Assessing the impact of new technology would be useful to compare different future policy scenarios, say, to reduce the environmental impacts of aviation.

The significant computational efficiency improvement offered by the approach presented in this paper would allow analyses to be performed that would otherwise be too expensive and impractical to perform, such as uncertainty and sensitivity analyses. Such analyses typically required performing the Monte Carlo simulations with thousands of runs. The sensitivity analysis would be particularly useful to evaluate future policy scenarios. For instance, the sensitivity analysis study could give insight into how the fuel burn performance would change with, say, the introduction of a new structural material (which would affect the weight) or a new engine (which would affect TSFC). This would provide the desired computational efficiency in decision-making and policy analyses.

Acknowledgements

This research did not receive any specific grant from funding agencies in the public, commercial, or not-for-profit sectors. Authors would like to thank the HKUST Post-Graduate International Student Fellowship Scheme for partially funding the first author.

References

AEDT, 2017. Aviation environmental design tool (aedt) technical manual, version 2d. U.S. Department of Transportation, Federal Aviation Administration.

Allaire, D., 2009. Uncertainty Assessment of Complex Models with Application to Aviation Environmental Systems. Ph.D. thesis. Massachusetts Institute of Technology.

Baughcum, S.L., Tritz, T.G., Henderson, S.C., Pickett, D.C., 1996. Scheduled Civil Aircraft Emission Inventories for 1992: Database Development and Analysis. NASA Contractor Report 4700.

Breguet, L., 1923. Calcul du Poids de Combustible Consummé par un Avion en Vol Ascendant. Comptes Rendus Hebdomodaires des Séances de l'Académie des Sciences 177, 870–872.

Casella, G., Berger, R.L., 2001. Statistical Inference. 2nd ed., Duxbury.

Chatterji, G.B., 2011. Fuel Burn Estimation Using Real Track Data, in: 11^{th} AIAA Aviation Technology, Integration, and Operations (ATIO) Conference, American Institute of Aeronautics and Astronautics. doi:10.2514/6.2011-6881.

Coffin, J.G., 1920. A Study of Airplane Range and Useful Loads. NACA-TR-69. NACA.

Dancila, B.D., Botez, R., Labour, D., 2013. Fuel burn prediction algorithm for cruise, constant speed and level flight segments. Aeronautical Journal 117, 491–504. doi:10.1017/S0001924000008149.

Diedrich, A., Hileman, J., Tan, D., Willcox, K., Spakovsky, Z., 2006. Multidisciplinary Design and Optimization of the Silent Aircraft, in: 44th AIAA Aerospace Sciences Meeting and Exhibit, Reno, NV. doi:10.2514/6.2006-1323. aIAA 2006-1323.

Graham, W.R., Hall, C.A., Vera-Morales, M., 2014. The potential of future aircraft technology for noise and pollutant emissions reduction. Transport policy 34, 36–51. doi:10.1016/j.tranpol.2014.02.017.

ICAO, 2010. Aviation and Climate Change. International Civil Aviation Organization (ICAO) Environmental Report.

ICAO, 2015. ICAO Carbon Emissions Calculator Methodology Version 8. https://www.icao.int/environmental-protection/CarbonOffset/Documents/Methodology%20ICAO%20Carbon%20Calculator_v8-2015.pdf (Last access: 28 July 2017).

ICAO, 2016. On board a sustainable future. International Civil Aviation Organization (ICAO) Enviromental Report.

IEA, 2008. World Energy Outlook 2008. International Energy Agency, Paris, France.

Kenway, G.K.W., Kennedy, G.J., Martins, J.R.R.A., 2012. A scalable parallel approach for high-fidelity aerostructural analysis and optimization, in: 53rd AIAA/ASME/ASCE/AHS/ASC Structures, Structural Dynamics, and Materials Conference, Honolulu, HI. AIAA 2012-1922.

Kim, B.Y., Fleming, G.G., Lee, J.J., Waitz, I.A., Clarke, J.P., Balasubramanian, S., Malwitz, A., Klima, K., Locke, M., Holsclaw, C.A., Maurice, L.Q., Gupta, M.L., 2007. System for assesing Aviation's Global Emissions (SAGE), Part 1: Model description and invertory results. Transportation Research Part D 12, 325–346. doi:10.1016/j.trd.2007.03.007.

Kroo, I.M., Sept 2006. Aircraft Design: Synthesis and Analysis. 1st ed., Desktop Aeronautics, Palo Alto, CA.

Lee, H., Chatterji, G.B., 2010. Closed-Form Takeoff Weight Estimation Model for Air Transportation Simulation, in: 10th AIAA Aviation Technology, Integration, and Operations (ATIO) Conference, Fort Worth, TX. doi:10.2514/6.2010-9156. AIAA 2010-9156.

Lee, J.J., 2010. Can we accelerate the improvement of energy efficiency in aircraft systems? Energy Conversion and Management 51, 189–196.

Lee, J.J., Lukachko, S.P., Waitz, I.A., Schafer, A., 2001. Historical future trends in aircraft performance, cost, and emissions. Annual Review of Energy and the Environment 26, 167–200. doi:10.1146/annurev.energy.26.1.167.

Liem, R.P., 2010. System Level Assessment of Uncertainty in Aviation Environmental Policy Impact Analysis. Master's thesis. Massachusetts Institute of Technology.

Liem, R.P., 2015. Multimission Fuel-Burn Minimization in Aircraft Design: A Surrogate-Modeling Approach. Ph.D. thesis. University of Toronto.

Liem, R.P., Kenway, G.K.W., Martins, J.R.R.A., 2015a. Multimission Aircraft Fuel Burn Minimization via Multipoint Aerostructural Optimization. AIAA Journal 53, 104–122. doi:10.2514/1.J052940.

Liem, R.P., Mader, C.A., Lee, E., Martins, J.R.R.A., 2013. Aerostructural design optimization of a 100-passenger regional jet with surrogate-based mission analysis, in: AIAA Aviation Technology, Integration, and Operations (ATIO) Conference, Los Angeles, CA. doi:10.2514/6.2013-4372.

Liem, R.P., Mader, C.A., Martins, J.R.R.A., 2015b. Surrogate models and mixtures of experts in aerodynamic performance prediction for mission analysis. Aerospace Science and Technology 43, 126–151. doi:10.1016/j.ast.2015.02.019.

Lloyd, S.P., 1982. Least Squares Quantization in PCM. IEEE Transactions on Information Theory 28, 129–137. doi:10.1109/TIT.1982.1056489.

MacQueen, J., 1967. Some methods for classification and analysis of multivariate observations, in: Fifth Berkeley Symposium on Mathematics. Statistics and Probability.. University of California Press., pp. 281–297.

McCormick, B.W., 1979. Aerodynamics, Aeronautics, and Flight Mechanics. John Wiley & Sons, New York, US.

Montgomery, D.C., Runger, G.C., 2003. Applied Statistics and Probability for Engineers. John Wiley & Sons, Inc.

O'Kelly, M.E., 2012. Fuel burn and environmental implications of airline hub networks. Transportation Research Part D: Transport and Environment 17, 555–567.

Randle, W.E., Hall, C.A., Vera-Morales, M., 2011. Improved Range Equation Based on Aircraft Flight Data. Journal of Aircraft 48, 1291–1298. doi:10.2514/1.C031262.

Rojo, J.J., 2007. Future trends in local air quality impacts of aviation. Master's thesis. Massachusetts Institute of Technology.

Roskam, J., 1985. Airplane Design Part I: Preliminary Sizing of Airplanes. Roskam Aviation and Engineering Corporations, Ottawa, KS.

Saltelli, A., Ratto, M., Andres, T., Campolongo, F., Cariboni, J., Gatelli, D., Saisana, M., Tarantola, S., 2008. Global Sensitivity Analysis: The Primer. John Wiley & Sons, Ltd., UK.

Simos, D., Jenkinson, L.R., 1988. Optimization of the Conceptual Design and Mission Profiles of Short-Haul Aircraft. Journal of Aircraft 25, 618–624.

Singh, V., Sharma, S.K., 2015. Fuel consumption optimization in air transport: a review, classification, critique, simple meta-analysis, and future research implications. European Transport Research Review 7, 1–24. doi:10.1007/s12544-015-0160-x.

Sokal, R.R., Rohlf, F.J., 2012. Biometry. 4th ed., Freeman.

Steinhaus, H., 1956. Sur la division des corps materiels en parties. Bull. Acad. Polon. Sci. 1, 801–804.

The World Bank, 2016. Air transport, passengers carried. http://data.worldbank.org/indicator/IS.AIR.PSGR?end=2016&locations=US&start=2000&view=chart&year=2016 (Last accessed: 26 July 2017).

Waitz, I., Lukachko, S., Willcox, K., Belobaba, P., Garcia, E., Hollingsworth, P., Mavris, D., Harback, K., Morser, F., Steinbach, M., 2006. Architecture Study for the Aviation Environmental Portfolio Management Tool. Partnership for Air Transportation Noise and Emissions Reduction PARTNER, Report No.: PARTNER-COE-2006-002.

Wasiuk, D.K., Lowernberg, M.H., Shallcross, D.E., 2015. An aircraft performance model implementation for the estimation of global and regional commercial aviation fuel burn and emissions. Transportation Research Part D 35, 142–159. doi:10.1016/j.trd.2014.11.022.

Yan, B., Jansen, P.W., Perez, R.E., 2012. Multidisciplinary Design Optimization of Airframe and Trajectory Considering Cost and Emissions, in: 14th AIAA/ISSMO Multidisciplinary Analysis and Optimization (MAO) Conference, Indianapolis, IN. doi:10.2514/6.2012-5494. AIAA 2012-5494.

Yanto, J., Liem, R.P., 2017. Efficient Fast Approximation for Aircraft Fuel Consumption for Decision-Making and Policy Analysis, in: AIAA Modeling and Simulation Technologies Conference, AIAA AVIATION Forum, Denver, Colorado. doi:10.2514/6.2017-3338.

Zady, M.F., . Z-4: Mean, Standard Deviation, and Coefficient of Variation. https://www.westgard.com/lesson34.htm [last accessed: April 22, 2017].